

Lanthanide complexes with zwitterionic amidoximes stabilized by noncoordinating water molecules

Steven P. Kelley & Robin D. Rogers

To cite this article: Steven P. Kelley & Robin D. Rogers (2017): Lanthanide complexes with zwitterionic amidoximes stabilized by noncoordinating water molecules, *Supramolecular Chemistry*, DOI: [10.1080/10610278.2017.1405002](https://doi.org/10.1080/10610278.2017.1405002)

To link to this article: <https://doi.org/10.1080/10610278.2017.1405002>

 View supplementary material 

 Published online: 26 Nov 2017.

 Submit your article to this journal 

 View related articles 

 View Crossmark data 



Lanthanide complexes with zwitterionic amidoximes stabilized by noncoordinating water molecules*

Steven P. Kelley^{a,b}  and Robin D. Rogers^{a,b,c} 

^aDepartment of Chemistry, The University of Alabama, Tuscaloosa, AL, USA; ^bDepartment of Chemistry, McGill University, Montreal, Canada; ^c525 Solutions, Inc., Tuscaloosa, AL, USA

ABSTRACT

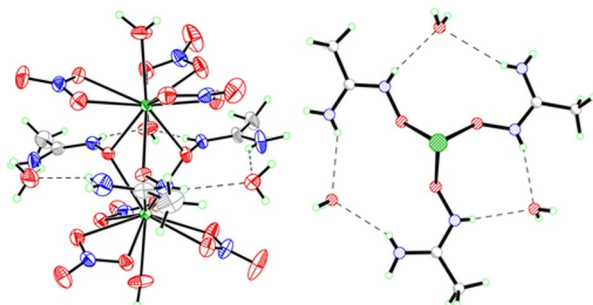
We present the first structural report of lanthanides complexed with free amidoxime ligands as part of our ongoing research effort to understand the interactions of amidoximes with metal ions in seawater. Three isomorphous lanthanide complexes with acetamidoxime (AcAO) having the formula $\text{Ln}_2(\text{NO}_3)_6(\text{AcAO})_3(\text{OH}_2)_3 \cdot 3\text{H}_2\text{O}$ ($\text{Ln} = \text{Pr}^{3+}, \text{Nd}^{3+}, \text{Gd}^{3+}$) have been crystallized and structurally characterised. Notably, the AcAO ligands coordinate in a bridging mode as zwitterions, which creates pre-organised hydrogen bonding cavities into which water molecules are incorporated. Charge-assisted hydrogen bonds to these water molecules appear to stabilize the zwitterionic form and thus the overall complex, underscoring the importance of supramolecular phenomena and overall complex geometry on the relative stability of amidoxime complexes. This has implications for controlling their selectivity towards metal ions.

ARTICLE HISTORY

Received 31 August 2017
Accepted 6 November 2017

KEYWORDS

Coordination chemistry;
f-elements; amidoxime;
hydrogen bonding



Introduction

There has been a recent rise in interest in the coordination chemistry of the amidoxime functional group ($\text{R}-\text{C}(\text{NH}_2)=\text{N}-\text{OH}$), notably due to its use in selective sorbents for the extraction of uranium from seawater (1). Amidoxime-functionalized resins have been demonstrated to extract uranium directly from the marine environment (2), but despite a number of improvements in capacity (3), recyclability (4, 5), and potential elimination of non-renewable chemicals from the process (6), they are not yet cost-competitive with terrestrial mining (7). The capacity of these sorbents could be greatly improved by increasing

their selectivity, as seawater contains many other metal ions at much higher concentrations than uranium. Some alternatives to amidoximes have recently been demonstrated at the laboratory scale, including anionic MOFs for capturing uranyl ($[\text{UO}_2]^{2+}$) ions (8) and cationic amine resins for capturing anionic complexes (9, 10). However, the leading strategy has been to improve the selectivity of amidoximes starting by understanding their interactions with metal ions, particularly $[\text{UO}_2]^{2+}$.

It has been established through a number of structural studies that amidoximes can exchange protons for $[\text{UO}_2]^{2+}$ to form η^2 complexes, as shown in Figure 1(a) and (b) (11,

CONTACT Robin D. Rogers  rdrogers@ua.edu

*Dedicated to Prof. Jerry L. Atwood for his 75th birthday.

 Supplemental data for this article can be accessed at <https://doi.org/10.1080/10610278.2017.1405002>.

© 2017 Informa UK Limited, trading as Taylor & Francis Group

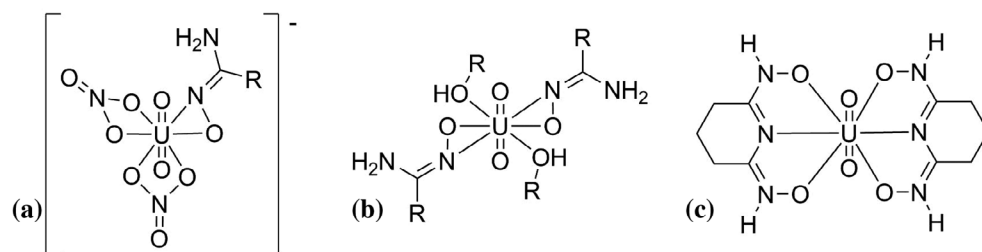


Figure 1. Coordination modes of amidoximate and imidedixioime.

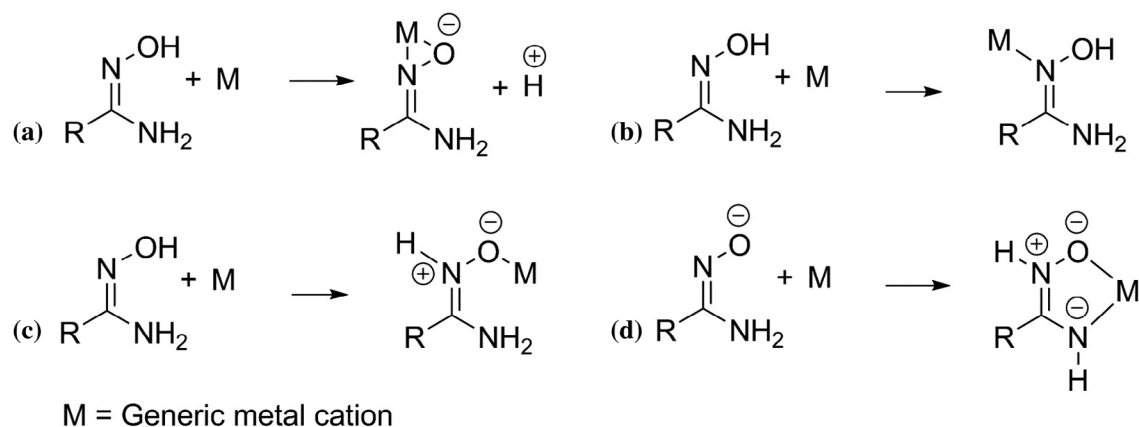


Figure 2. General reactions of amidoximes or amidoximates with metal ions.

12). This coordination mode has only been observed for complexes of amidoximate with $[\text{UO}_2]^{2+}$ or $\text{Mo}^{4+/6+}$ (13). Adjacent amidoxime groups on a polymer can also react with each other to form a chelating imide dioxime which is usually believed to be a more active binding site for $[\text{UO}_2]^{2+}$ than the amidoxime itself (14). These chelate $[\text{UO}_2]^{2+}$ through the O and central N atoms (15), forming a cycle (Figure 1(c)). Again, this chelating mode is very reasonable for $[\text{UO}_2]^{2+}$, which can readily accommodate six equatorial coordinating atoms, but would be unusual for a smaller or more spherical metal ion.

Improving selectivity for $[\text{UO}_2]^{2+}$ requires not only increasing the strength of its interactions with amidoxime but also inhibiting the interactions with other metal ions. Experimentally determined amidoxime coordination modes have been recently reviewed by Bolotin et al. (13). Whereas the η^2 coordination of $[\text{UO}_2]^{2+}$ occurs through cation exchange (Figure 2(a)), as this coordination mode greatly increases the acidity of the oxime group (16), other metal ions can coordinate to amidoxime without cation exchange by metallating the oxime N atom (Figure 2(b)) or the O atom of the zwitterionic tautomer (Figure 2(c)). Even the amidoximate anion is capable of tautomerization, and the chelating amidinate tautomer (Figure 2(d)) interacts more strongly with $[\text{VO}]^{2+}$ than amidoximate does with $[\text{UO}_2]^{2+}$ (17). These observations suggest that controlling protonation of amidoximes, particularly at the N position,

could be a mechanism for eliminating competition from a broad range of metal ions.

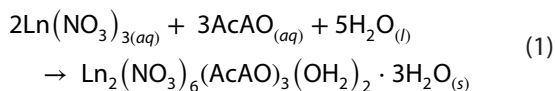
In practice, major improvements in sorbent performance are often accomplished without modifying the moiety of the extractant that actually coordinates to the metal ion. These approaches include grafting amidoxime groups onto ultra-high surface area porous aromatic frameworks to increase capacity (18) or crosslinking known extractant moieties with hydrophilic acrylamide linkers to improve uptake kinetics (19). Such systems involve noncovalent or cooperative effects dictated by the relative positions of functional groups which are difficult to understand by techniques that look at molecular structure, but our group has found that crystal structure determination by single crystal X-ray diffraction (SCXRD) on carefully chosen models of such systems can capture some of the phenomena which are occurring. For instance, we have previously shown through crystal structures of metal complexes that $[\text{UO}_2]^{2+}$ -amidoxime interactions could be stabilized through noncovalent, cooperative interactions with a pendant cation (11) and that $[\text{UO}_2]^{2+}$ could be chelated by adjacent amidoximes in a 1,2-position (20).

In our present study, we investigate the interactions of trivalent lanthanides (Ln^{3+}) with acetamidoxime (AcAO), a simple monoamidoxime ligand with no other coordinating functional groups. Only two structures have ever been reported which contain Ln^{3+} ions interacting with

amidoximate ions, both of which are mixed $\text{Ln}^{3+}/\text{Ni}^{2+}$ complexes where anionic Ni^{2+} amidoximate complexes act as chelators, rather than the amidoxime ligands themselves (21, 22). We expected that Ln^{3+} ions would be useful for understanding structural features which can be attributed to the unusually strong interaction between $[\text{UO}_2]^{2+}$ and amidoximes, since Ln^{3+} ions overlap with $[\text{UO}_2]^{2+}$ in size, but lack these interactions. Additionally, $[\text{UO}_2]^{2+}/\text{Ln}^{3+}$ separations are relevant in non-seawater applications such as the use of amidoxime sorbents to recover uranium from spent nuclear fuel processing streams (23). We sought to begin our investigation of this under-explored system by crystallizing complexes formed from the reaction of $\text{Ln}(\text{NO}_3)_3 \cdot 6\text{H}_2\text{O}$ ($\text{Ln} = \text{Nd}, \text{Gd}, \text{or Pr}$) and AcAO.

Results and discussion

Crystals of $\text{Ln}_2(\text{NO}_3)_6(\text{AcAO})_3(\text{OH}_2)_2 \cdot 3\text{H}_2\text{O}$ were formed by reacting aqueous solutions of the corresponding lanthanide nitrate hexahydrate and AcAO (Equation (1)). Combining the solutions did not result in any precipitate, nor did any solids form upon vapor diffusion of acetone into the resulting solutions. The compounds were ultimately crystallized by allowing the acetone-water mixtures to evaporate to dryness under ambient conditions, yielding crusts of different coloured solids depending on the metal (green for Pr^{3+} , pink for Nd^{3+} , and colourless for Gd^{3+}). Single crystals were isolated directly from these reaction mixtures and analyzed by SCXRD.



All three compounds were isomorphous and crystallized in the face-centred orthorhombic space group $Fdd2$ with $Z' = 0.5$. The $\text{Ln}_2(\text{NO}_3)_6(\text{AcAO})_3(\text{OH}_2)_2$ molecules are

discrete, neutral, dinuclear complexes residing on crystallographic 2-fold axes which pass through one of the AcAO ligands (Figure 3). The 2-fold symmetry causes the two Ln^{3+} centres to be identical, relates two of the AcAO ligands to each other, and causes the third to be disordered over two symmetry related positions. There are three non-coordinating water molecules per $\text{Ln}_2(\text{NO}_3)_6(\text{AcAO})_3(\text{OH}_2)_2$, two of which are related by symmetry and one of which sits on the 2-fold axis.

The metal centres have coordination numbers of 10 and are coordinated to three bidentate $[\text{NO}_3]^-$ ions, one water molecule, and three bridging AcAO ligands (Figure 4). The coordination geometry is highly distorted from ideal polyhedral and can be described as a capped trigonal cupola, as observed for 10-coordinate Pu^{3+} in polyborate networks (24). Each $[\text{NO}_3]^-$ ion chelates unsymmetrically, which is typical for lanthanide nitrate complexes. The AcAO ligands bridge two metal centres solely through the oxygen atom, so that the coordination polyhedra of the two metals are face-sharing.

The AcAO ligands are in a zwitterionic tautomeric form, also seen in the crystal structure of $\text{UO}_2(\text{NO}_3)_2(\text{AcAO})_2$ (25). The manner in which their negatively charged oxygen atoms bridge the Ln^{3+} centres is similar to that observed in crystal structures of binuclear, face-sharing lanthanide complexes bridged by alkoxides (26, 27). In all of these structures, the μ^2 -oxygen atoms are pyramidal, rather than planar. Two of the pyramids are oriented with their vertices 120° to each other, presumably minimising repulsion of the nonbonding lone pair located there. The third oxygen atom can only have this orientation relative to one of the neighbours but not both, and the resulting frustration appears to give rise to the disorder in the AcAO ligand. The similarity of the bridging oxygen atoms in $\text{Ln}_2(\text{NO}_3)_6(\text{AcAO})_3(\text{OH}_2)_2$ to alkoxides indicates a high degree of charge separation between the N and O. Thus,

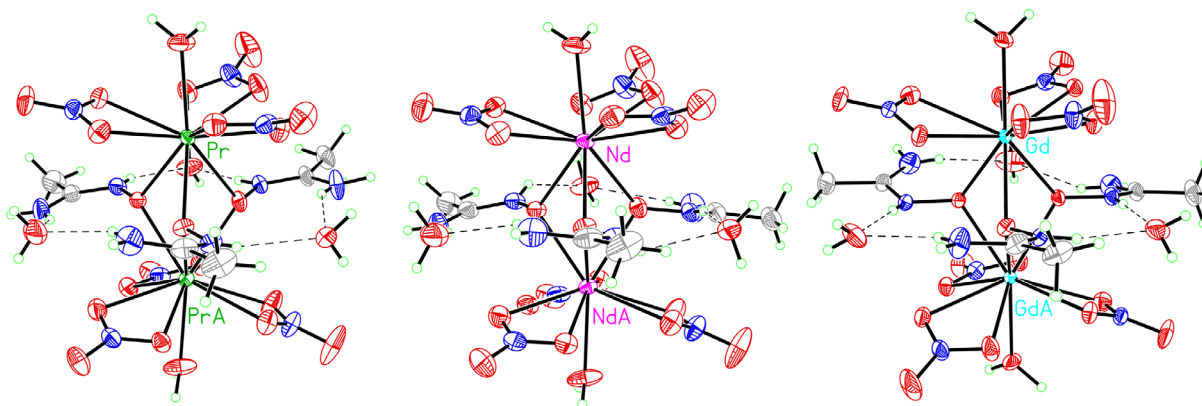


Figure 3. (Colour online) Fifty per cent probability ellipsoid plots of $\text{Pr}_2(\text{NO}_3)_6(\text{AcAO})_3(\text{OH}_2)_2 \cdot 3\text{H}_2\text{O}$ (left), $\text{Nd}_2(\text{NO}_3)_6(\text{AcAO})_3(\text{OH}_2)_2 \cdot 3\text{H}_2\text{O}$ (centre), and $\text{Gd}_2(\text{NO}_3)_6(\text{AcAO})_3(\text{OH}_2)_2 \cdot 3\text{H}_2\text{O}$ (right), emphasising the isostructural nature of the complexes. Dashed lines indicate shortest intermolecular interactions.

Note: Disorder omitted for clarity.

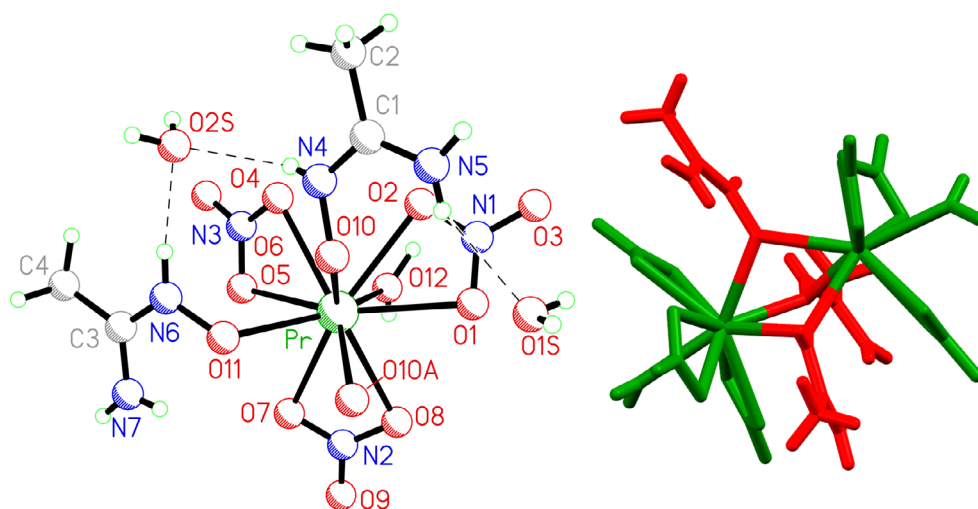


Figure 4. (Colour online) *Left:* Labeled ball and stick plot of asymmetric unit of $\text{Pr}_2(\text{NO}_3)_6(\text{AcAO})_3(\text{OH}_2)_2 \cdot 3\text{H}_2\text{O}$ with symmetry equivalent atoms added to show full metal coordination sphere. Dashed lines indicate shortest intermolecular interactions. O10A is the symmetry equivalent of AcAO oxygen atom O10. *Right:* Stick plot emphasising the shared face.

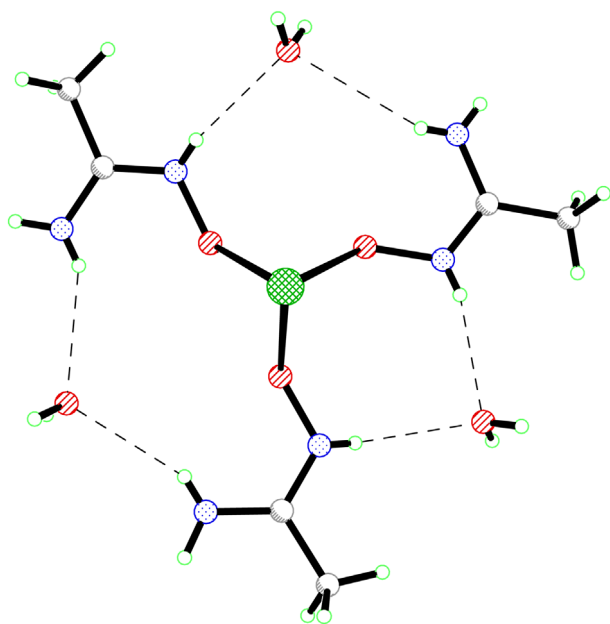


Figure 5. (Colour online) Ball and stick plot showing hydrogen bonding of lattice water molecules to zwitterionic AcAO ligands.

it is the ability of amidoxime to coordinate as a zwitterion which stabilizes these particular complexes, and the factors which stabilize the zwitterion warrant investigation.

While lattice water molecules appear to be common in, for instance, uranyl amidoximate complexes, the coordination geometry of $\text{Ln}_2(\text{NO}_3)_6(\text{AcAO})_3(\text{OH}_2)_2$ produces an exceptional situation. The geometry of the complex pre-organises the AcAO zwitterions into cavities which are ideally suited for donating hydrogen bonds to a single water molecule. This gives rise to the large hydrogen bonded cycle shown in Figure 5. Each of these hydrogen bonds is a strong and in some cases charge-assisted

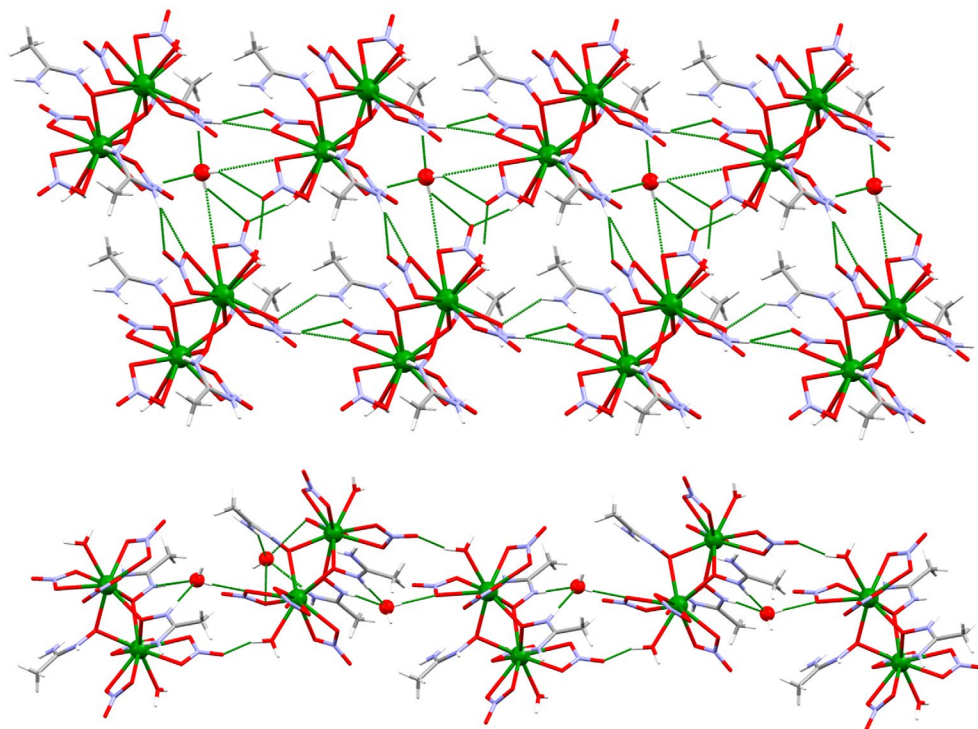
interaction, and the ability of the complex to form six such interactions while adopting an undistorted geometry preferred by lanthanide alkoxide complexes is likely a source of significant additional stabilization. The hydrogen bonding to water also has the consequence of reducing homomolecular hydrogen bonding between AcAO ligands, which would weaken the metal-ligand interaction of the hydrogen bond acceptor.

There are no other lanthanide amidoxime structures to determine by comparison if the hydrogen bonding to water molecules affects the metal-AcAO interaction. However, the hydrogen bonding patterns in the crystal structure do suggest that water molecules are delocalizing some of the positive charge from the AcAO nitrogen centres. All water molecules act as hydrogen bond donors, as well as Lewis bases, either by coordinating to the metal ion or accepting hydrogen bonds. Water molecules ligated to the metal centre donate the shortest hydrogen bonds out of any water molecules in the structure, noncoordinating water molecules interacting with the iminium nitrogen donate the next shortest, and those interacting only with amide groups donate long, bifurcated hydrogen bonds (Table 1). This suggests that the water molecules which interact with more acidic sites are themselves more acidic, whether it be through coordination to the metal ion or hydrogen bonding to the zwitterionic amidoxime.

Lattice water molecules also often play an important role in stabilizing the packing of crystals by forming hydrogen bonded networks which buffer effects such as size mismatches between ions and offer additional interactions with polar functional groups. However, it can be seen in Figure 6 that the $\text{Ln}_2(\text{NO}_3)_6(\text{AcAO})_3(\text{OH}_2)_2$ complexes form a hydrogen bonded network on their own, and the lattice

Table 1. Hydrogen bond donor-to-acceptor (O...O) distances in Å for hydrogen bonds donated by the water molecules in $\text{Ln}_2(\text{NO}_3)_6(\text{AcAO})_3(\text{OH}_2)_2 \cdot 3\text{H}_2\text{O}$.

Bond	$\text{Pr}_2(\text{NO}_3)_6(\text{AcAO})_3(\text{OH}_2)_2 \cdot 3\text{H}_2\text{O}$	$\text{Nd}_2(\text{NO}_3)_6(\text{AcAO})_3(\text{OH}_2)_2 \cdot 3\text{H}_2\text{O}$	$\text{Gd}_2(\text{NO}_3)_6(\text{AcAO})_3(\text{OH}_2)_2 \cdot 3\text{H}_2\text{O}$
Coordinated water molecules			
O12...O6	2.705(4)	2.711(6)	2.732(4)
O12...O9	2.751(3)	2.758(5)	2.762(4)
Water molecules accepting iminium hydrogen bonds			
O15...O1	2.836(4)	2.828(5)	2.820(4)
O15...O3	2.937(4)	2.934(6)	2.932(4)
Water molecules accepting only amide hydrogen bonds			
O25...O7	3.302(4)	3.305(6)	3.323(4)
O25...O9	3.325(5)	3.321(8)	3.293(6)

**Figure 6.** (Colour online) Hydrogen bond motifs between $[\text{NO}_3]^-/\text{AcAO}$ groups (*top*) and $[\text{NO}_3]^-/\text{OH}_2$ ligands (*bottom*), both reinforced by interactions with lattice water molecules, in $\text{Ln}_2(\text{NO}_3)_6(\text{AcAO})_3(\text{OH}_2)_2 \cdot 3\text{H}_2\text{O}$.

water molecules simply support that network without creating any new hydrogen bonded bridges. The structure packs by forming a dense hydrogen bonded network. Infinite layers form perpendicular to the a axis through hydrogen bonds between the water molecule occupying the 2-fold axis and the nitrate groups of adjacent molecules (Figure 6, *top*). These layers are reinforced by hydrogen bonds from the amide groups and coordinated water molecules. The layers interact along a through more hydrogen bonds involving the lattice water molecules and nitrate groups (Figure 6, *bottom*). As the water molecules have only an ancillary role in the packing, this further supports that they are incorporated in the structure due to the strength of their interactions with the complex rather than as just waters of crystallization.

Conclusions

The first crystal structures of lanthanide ions with free amidoxime ligands, $\text{Ln}_2(\text{NO}_3)_6(\text{AcAO})_3(\text{OH}_2)_2 \cdot 3\text{H}_2\text{O}$ have been described. As hard acids, lanthanides prefer to coordinate with the anionic oxygen atom of the zwitterionic form of AcAO. However, the preferred geometry for such a complex also creates three pre-organised hydrogen-bonding cavities per complex, resulting in the crystallization of a trihydrate. These hydrogen bonds further strengthen the metal-ligand interaction through stabilization of the zwitterion and donation of additional electron density to the ligand.

The protonation state of amidoxime, particularly at the imine nitrogen atom, has been shown to be a key factor in how it coordinates. These new structures present

evidence for the extent to which supramolecular interactions can stabilize the zwitterionic form of an amidoxime, which would in turn prevent the proton exchange reaction needed for irreversible adsorption. Such phenomena are related to structural elements, such as the overall geometry of a metal-amidoxime complex, which are under-investigated compared to the metal-amidoxime interaction itself. A better understanding of how factors such as hydration of the metal complexes affect their stability could lead to ligand design strategies which augment the selectivity of amidoxime-based sorbents for uranium ions without changing the fundamental nature of the amidoxime-metal interaction. For instance, the hydrogen bonds in $\text{Ln}_2(\text{NO}_3)_6(\text{AcAO})_3(\text{OH}_2)_2 \cdot 3\text{H}_2\text{O}$ could be inhibited by changing the functional groups at noncoordinating positions of the ligand (such as the R groups of the noncoordinating amide), allowing the selectivity of amidoxime to be tuned without changing the fundamental nature of its interaction with metal ions.

The ability to stabilize or destabilise protonation of the N and O positions of the oxime group may prove to be a tool for improving selectivity for $[\text{UO}_2]^{2+}$ since it affects the availability of these sites for coordination. Since $[\text{UO}_2]^{2+}$ coordinates to both atoms of an oximate anion, while the ions that outcompete it such as Na^+ and $\text{V}^{4+/5+}$ coordinate only to one of the atoms, the protonation states of amidoxime groups likely have a role in selectivity that is not yet fully understood.

Experimental

Materials and methods

Acetonitrile (EMD Chemicals, Billerica, MA), hydroxylamine (50 wt.% solution in water, Alfa-Aesar, Ward Hill, MA), and $\text{Ln}(\text{NO}_3)_3 \cdot 6\text{H}_2\text{O}$ (Strem Chemical, Newburyport, MA) were used as received from their commercial sources. Deionized water was obtained from an in-house deionizer system (Culligan International Co., Rosemont, IL; typical resistivity 17.8 $\text{M}\Omega\cdot\text{cm}$). ^1H NMR was measured using a Bruker Avance 300 MHz NMR spectrometer (Bruker Corporation, Billerica, MA). Infrared spectroscopy was measured using a Bruker ALPHA FT-IR with an ATR accessory (Bruker Optics, Billerica, MA). SCXRD was measured using a Bruker diffractometer equipped with a 3-circle PLATFORM goniometer and an Apex II CCD area detector (Bruker-AXS, Madison, WI).

Synthesis of AcAO

AcAO was synthesised according to a published procedure (28). Acetonitrile and 50 wt.% hydroxylamine in water were separately mixed with methanol and combined at a 1:1 M ratio of acetonitrile to hydroxylamine. The reaction mixture was stirred for 48 h at room temperature. Solvent was

removed by rotary evaporation to give a white powder, which was re-dissolved in hot methanol and recrystallized on standing overnight to give long, colourless prisms of AcAO. ^1H NMR (300 MHz, $\text{dms}\text{-}d_6$) δ : 8.65 (s, =N-OH), 5.34 (s, -NH₂), 1.61 (s, -CH₃). IR (cm^{-1} , neat sample in ATR mode): 3490 (m), 3366 (m), 3153 (m, br), 2769 (m), 1653 (s), 1586 (s), 1433 (w), 1393 (s), 1364 (m), 1104 (w, br), 1047 (w), 1021 (w), 891 (s), 816 (m, br).

Crystallization of lanthanide-AcAO complexes

$\text{Ln}_2(\text{NO}_3)_6(\text{AcAO})_3(\text{OH}_2)_2 \cdot 3\text{H}_2\text{O}$

Approximately 50 mg each of $\text{Ln}(\text{NO}_3)_3 \cdot 6\text{H}_2\text{O}$ salt was dissolved in 200–300 μL of deionized water. Three molar equivalents of AcAO were weighed out, dissolved completely in deionized water, and added to the $\text{Ln}(\text{NO}_3)_3$ solutions. The mixtures were sealed in vials containing *ca.* 1 mL of acetone, which transferred completely into the aqueous solution through vapor diffusion without any precipitation occurring. The water/acetone solutions were then allowed to evaporate under ambient conditions. Crystals for structure determination were obtained after *ca.* 1 month.

Crystal structure determination

Crystals were selected under an optical polarising microscope, mounted on a glass fibre with silicone grease, and cooled to the collection temperature under a stream of cold nitrogen using an Oxford N-Helix cryostat (Oxford Cryosystems, Oxford, UK). A strategy of scans about the omega and phi axes were used to collect a hemisphere of unique data for each crystal under Mo-K α radiation ($\lambda = 0.71073 \text{ \AA}$). Data collection, unit cell determination, integration, scaling, and absorption correction were all performed using the Bruker Apex2 software suite (29).

All three structures were solved by direct methods. The metal atom site was initially located and refined, and all remaining non-hydrogen atoms were located from the difference map. All non-hydrogen atoms were refined anisotropically by full matrix least squares refinement against F^2 . All structures contained an AcAO ligand which was disordered by symmetry over two positions and whose site occupancy factors were therefore fixed at 50%. Hydrogen atoms bonded to strong hydrogen bond donors were located from the difference map. The positions of these hydrogen atoms were freely refined, while their thermal parameters were constrained to ride on the carrier atom. It was found that these hydrogen atoms converged to positions that were realistic based on molecular geometry and the positions of nearby hydrogen bond acceptors, although they often refined to unrealistic N–H or O–H bond distances. This is a typical error for hydrogen atom positions that are refined against hard X-ray data collected on a heavy-atom

containing structure. It was determined unnecessary to add further restraints or constraints to these hydrogen atoms since they converged to positions that effectively illustrated the hydrogen bonding and protonation states of the structure. There is a false B-level CheckCIF alert for one of the lattice water molecules in $\text{Pr}_2(\text{NO}_3)_6(\text{AcAO})_3(\text{OH}_2)_2 \cdot 3\text{H}_2\text{O}$ lacking a hydrogen bond acceptor. This molecule donates a bifurcated hydrogen bond which is missed by the test due to the criteria for linearity of the $\text{O-H} \cdots \text{X}$ bond.

Space group determination, structure solution and refinement, and the generation of ORTEP plots were implemented using the Bruker SHELXTL software suite (30). The structures were refined using SHELXL-v.2014 (31). Short contact analysis and packing plots were done using Mercury 3.9 (Cambridge Crystallographic Data Centre, Cambridge, UK) (32).

Acknowledgements

The authors would like to thank the U.S. DOE Office of Nuclear Energy Nuclear Energy University Programs (grant number DE-NE0000672) and the Natural Sciences and Engineering Research Council of Canada (Discovery Grant RGPIN-2016-04944) for support of this work. This research was undertaken, in part, thanks to funding from the Canada Excellence Research Chairs program.

Disclosure statement

No potential conflict of interest was reported by the authors.

Funding

This work was supported by the U.S. DOE Office of Nuclear Energy Nuclear Energy University Programs [grant number DE-NE0000672] and the Natural Sciences and Engineering Research Council of Canada [Discovery grant number RGPIN-2016-04944] and in part, from the Canada Excellence Research Chairs Program.

ORCID

Steven P. Kelley  <http://orcid.org/0000-0001-6755-4495>

Robin D. Rogers  <http://orcid.org/0000-0001-9843-7494>

References

- Kim, J.; Tsouris, C.; Mayes, R.T.; Oyola, Y.; Saito, T.; Janke, C.J.; Dai, S.; Schneider, E.; Sachde, D. *Sep. Sci. Technol.* **2013**, *48*, 367–387.
- Seko, N.; Katakai, A.; Hasegawa, S.; Tamada, M.; Kasai, N.; Takeda, H.; Sugo, T.; Saito, K. *Nucl. Technol.* **2003**, *144*, 274–278.
- Oyola, Y.; Janke, C.J.; Dai, S. *Ind. Eng. Chem. Res.* **2016**, *55*, 4149–4160.
- Pan, H.-B.; Liao, W.; Wai, C.M.; Oyola, Y.; Janke, C.J.; Tian, G.; Rao, L. *Dalton Trans.* **2014**, *43*, 10713–10718.
- Berton, P.; Kelley, S.P.; Rogers, R.D. *Ind. Eng. Chem. Res.* **2016**, *55*, 4321–4327.
- Barber, P.S.; Kelley, S.P.; Griggs, C.S.; Wallace, S.P.; Rogers, R.D. *Green Chem.* **2014**, *16*, 1828–1836.
- Flicker Byers, M.; Schneider, E. *Ind. Eng. Chem. Res.* **2016**, *55*, 4351–4361.
- Carboni, M.; Abney, C.W.; Liu, S.; Lin, W. *Chem. Sci.* **2013**, *4*, 2396–2402.
- Sellin, R.; Alexandratos, S.D. *Ind. Eng. Chem. Res.* **2013**, *52*, 11792–11797.
- Guo, X.; Huang, L.; Li, C.; Hu, J.; Wu, G.; Huai, P. *Phys. Chem. Chem. Phys.* **2015**, *17*, 14662–14673.
- Barber, P.S.; Kelley, S.P.; Rogers, R.D. *RSC Adv.* **2012**, *2*, 8526–8530.
- Vukovic, S.; Watson, L.A.; Kang, S.O.; Custelcean, R.; Hay, B.P. *Inorg. Chem.* **2012**, *51*, 3855–3859.
- Bolotin, D.S.; Bokach, N.A.; Kukushkin, V.Yu. *Coord. Chem. Rev.* **2016**, *313*, 62–93.
- Astheimer, L.; Schenk, H.J.; Witte, E.G.; Schwochau, K. *Sep. Sci. Technol.* **1983**, *18*, 307–339.
- Tian, G.; Teat, S.J.; Zhang, Z.; Rao, L. *Dalton Trans.* **2012**, *41*, 11579–11586.
- Kukushkin, V.Yu.; Tudela, D.; Pomeiro, A.J.L. *Coord. Chem. Rev.* **1996**, *156*, 333–362; Macrae, C.F.; Bruno, J.I.; Chisholm, J.A.; Edgington, P.R.; McCabe, P.; Pidcock, E.; Rodriguez-Monge, L.; Taylor, R.; van de Streek, J.; Wood, P.A. *J. Appl. Cryst.* **2008**, *41*, 466–470.
- Mehio, N.; Johnson, J.C.; Dai, S.; Bryantsev, V.S. *Phys. Chem. Chem. Phys.* **2015**, *17*, 31715–31726.
- Li, B.; Sun, Q.; Abney, C.W.; Aguila, B.; Lin, W.; Ma, S. *ACS Appl. Mater. Interfaces* **2017**, *9*, 12511–12517.
- Piechowicz, M.; Abney, C.W.; Thacker, N.C.; Gilhula, J.C.; Wang, Y.; Veroneau, S.; Hu, A.; Lin, W. *ACS Appl. Mater. Interfaces* **2017**, *9*, 27894–27904.
- Kelley, S.P.; Barber, P.S.; Mullins, P.H.K.; Rogers, R.D. *Chem Commun.* **2014**, *50*, 12504–12507.
- Dong, H.M.; Li, Y.; Yang, E.-C.; Zhao, X.-J. *Dalton Trans.* **2016**, *45*, 11876–11882.
- Kalogridise, C.; Palacios, M.A.; Rodríguez-Diéguez, A.; Mota, A.J.; Choquesillo-Lazarte, D.; Brechin, E.K.; Colacio, E. *Eur. J. Inorg. Chem.* **2011**, 5225–5232.
- Nogami, M.; Kim, S.-Y.; Asanuma, N.; Ikeda, Y.J. *Alloys. Compd.* **2004**, *374*, 269–271.
- Wang, S.; Alekseev, E.V.; Depmeier, W.; Albrecht-Schmitt, T.E. *Inorg. Chem.* **2011**, *50*, 2079–2081.
- Witte, E.G.; Swochau, K.S.; Henkel, G.; Krebs, R. *Inorg. Chim. Acta* **1984**, *94*, 323–331.
- Schläfer, J.; Tyrre, W.; Mathur, S. *Inorg. Chem.* **2014**, *53*, 2571–2753.
- Thiakou, K.A.; Nastopoulos, V.; Terzis, A.; Raptopoulou, C.P.; Perlepes, S.P. *Polyhedron* **2006**, *25*, 539–549.
- Hirotsu, T.; Katoh, S.; Sugasaka, K.; Senō, M.; Itagaki, T. *J. Chem. Soc. Dalton Trans.* **1986**, 1609–1611.
- APEX 2 AXScale and SAINT, version 2010; Bruker AXS Inc: Madison, WI, **2010**.
- Sheldrick, G.M. *SHELXTL, structure determination software suite, v. 6.10*; Bruker AXS Inc: Madison, WI, **2001**.
- Sheldrick, G.M. *Acta Cryst. Sect. A Found. Crystallogr.* **2015**, *71*, 3–8.
- Macrae, C.F.; Bruno, J.I.; Chisholm, J.A.; Edgington, P.R.; McCabe, P.; Pidcock, E.; Rodriguez-Monge, L.; Taylor, R.; van de Streek, J.; Wood, P.A.J. *J. Appl. Cryst.* **2008**, *41*, 466–470.